Eur. Phys. J. B **23**, 391–404 (2001)

THE EUROPEAN PHYSICAL JOURNAL B

EDP Sciences

A wave automaton for Maxwell's equations

C. Vanneste[a]

Laboratoire de Physique de la Matière Condensée[b], Université de Nice-Sophia Antipolis, Parc Valrose, BP 71, 06108 Nice Cedex 2, France

Received 19 July 2001

Abstract. This paper presents an extension to electromagnetic fields of the wave automaton, which was introduced in recent years for describing wave propagation in inhomogeneous media. Using elementary processes obeying a discrete Huygens' principle and satisfying fundamental symmetries such as time reversal and reciprocity, this new wave automaton is capable of modeling Maxwell's equations in 3+1 dimensions. It supplements the methods that were developed early for scalar and spinor fields.

PACS. 03.50.De Classical electromagnetism, Maxwell equations – 42.25.Fx Diffraction and scattering – 02.70.-c Computational techniques

1 Introduction

The wave automaton is a numerical method devoted to wave propagation in random media [1,2]. Inspired from lattice gas automata, it introduces real or complex quantities that propagate along the bonds and scatter over the nodes of a discrete lattice. In this paper, we shall refer to these real or complex quantities as currents. Owing to the scattering processes at the lattice nodes, which is the counterpart of the collision rules in lattice gas automata, the wave automaton can be considered as a discrete modeling of Huygens' principle [3]. The currents are also similar (but not identical) to the voltage pulses of the Transmission Line Matrix Modeling method (TLM) which is commonly used to solve the Maxwell equations in electromagnetic structures [4]. Due to its construction, which is different from TLM and relies on fundamental symmetries of the time evolution of the currents such as time reversal and reciprocity [5,6], it turns out that the wave automaton is fully described by a network of unitary scattering matrices. Hence, it is affiliated to other models like the lattice Boltzmann wave model [7,8], quantum cellular automata [9,10], network models (NWM) [11,12]. Although also related to lattice gas automata, it differs from them since the currents are real or complex quantities instead of Boolean variables (see for instance the recent model for 3D electromagnetic propagation introduced in [13]).

In its previous versions, the wave automaton was shown to be able to describe the Schrödinger, the Klein-Gordon, the classical wave equations [6,14] and the Dirac equation [15]. In this paper, we will focus on the Maxwell's equations. In contrast with the scalar wave equations, two kinds of fields must be introduced, namely the electric field E and the magnetic field H. It will be shown that these two fields emerge naturally from the general rules, which govern the construction of the wave automaton. Moreover, the construction handles properly the vector nature of E and H by introducing their three Cartesian components in the classical Yee scheme [16].

The paper is organized as follows. In Section 2, we briefly recall the main steps of the construction along the lines described in [6]. This includes the definition of the currents and of the field, the propagation and scattering rules and their symmetries. We stress the importance of the special form of the scattering matrices, which is needed to close the wave equation. This result enables to eliminate the currents from the equation that governs the field evolution and makes the wave automaton equivalent to a finite-difference scheme. In Section 3, we point out the step of the construction, which differs from the scalar wave automaton and leads to the introduction of two interconnected kinds of fields. Due to their properties, these two fields can be identified with the electric and magnetic fields. The resulting wave automaton leads to the Maxwell's equations in inhomogeneous and anisotropic media. In conclusion, we discuss possible extensions of this work.

2 The general construction of the wave automaton

In this section, we introduce the definitions, notations and the main steps of the construction of a discrete wave equation.

2.1 Definition and evolution of the currents

The currents are defined as real numbers [17] that propagate along the bonds of a discrete lattice (Fig. 1a). The

[a] e-mail: vanneste@unice.fr
[b] CNRS UMR 6622

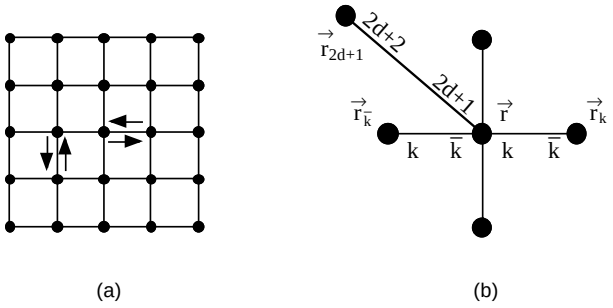

Fig. 1. (a) Propagation of currents along the bonds of a regular lattice. (b) The bonds are labeled $k = 1, \dots 2d+1$ at node $\mathbf{r}$ and $2d+2$ at node $\mathbf{r}_{2d+1}$. The neighbor node that is linked to $\mathbf{r}$ through bond k is referred to as $\mathbf{r}_k$. The bond labeled k at node $\mathbf{r}$ is given the label $\overline{k}$ at node $\mathbf{r}_k$. In particular, $2d+2 = \overline{2d+1}$ and $2d+1 = \overline{2d+2}$.

nodes of the lattice are labeled by the discrete vector positions $\mathbf{r}$. Although most of the results described in this section are valid over any arbitrary lattice, we shall consider in the following a cubic lattice in d dimensions. At each time t, $2d$ outgoing currents $s_k(\mathbf{r},t)$, $k = 1, \dots 2d$ leave each lattice node $\mathbf{r}$ and propagate in one discrete time step τ to the $2d$ neighbor nodes $\mathbf{r}_k$ where they become incident currents $e_{\overline{k}}(\mathbf{r}_k, t+\tau)$. We have used the following notations. Node $\mathbf{r}_k$ is the neighbor site, which is linked to node $\mathbf{r}$ by the bond k, along which the currents $e_k(\mathbf{r},t)$ and $s_k(\mathbf{r},t)$ propagate. Moreover, bond k for node $\mathbf{r}$ is referred to as bond $\overline{k}$ for node $\mathbf{r}_k$ (Fig. 1b). With this convention, the propagation step along the bond k of node $\mathbf{r}$ (or bond $\overline{k}$ of node $\mathbf{r}_k$) reads $e_{\overline{k}}(\mathbf{r}_k, t+\tau) = s_k(\mathbf{r},t)$ and $e_k(\mathbf{r}, t+\tau) = s_{\overline{k}}(\mathbf{r}_k, t)$. Note that since we consider a Cartesian lattice, the index k can be associated to a particular lattice direction and $\overline{k}$ to the opposite direction. This would not be true for a random lattice as considered for instance in [6].

An additional outgoing current $s_{2d+1}(\mathbf{r},t)$ leaves each node $\mathbf{r}$ at each time t. This current (hereafter referred as the on-site current) can be considered as propagating along a bond labeled $2d+1$ that is attached to the node. This bond does not connect node $\mathbf{r}$ to one of its neighbor nodes $\mathbf{r}_k$, $k = 1, \dots 2d$ but to a node $\mathbf{r}_{2d+1}$ that is attached to node $\mathbf{r}$ (Fig. 1). The label $2d+1$ is chosen for notational convenience although it does not refer to any spatial direction. This propagation step reads $e_{2d+2}(\mathbf{r}_{2d+1}, t+\tau) = s_{2d+1}(\mathbf{r},t)$ where $e_{2d+2}(\mathbf{r}_{2d+1}, t)$ is the incident current at node $\mathbf{r}_{2d+1}$ and at time t. The reverse propagating process from node $\mathbf{r}_{2d+1}$ to node $\mathbf{r}$ reads $e_{2d+1}(\mathbf{r}, t+\tau) = s_{2d+2}(\mathbf{r}_{2d+1}, t)$. According to our notation defined above, note that $\overline{2d+1} = 2d+2$ and $\overline{2d+2} = 2d+1$. All or a fraction of the current $s_{2d+1}(\mathbf{r},t)$, which leaves node $\mathbf{r}$ at time t and becomes an incident current at node $\mathbf{r}_{2d+1}$ at time $t+\tau$, will be sent back to node $\mathbf{r}$ at time $t+2\tau$ after a scattering process to be described below. This additional propagation step on bond $2d+1$ is equivalent to the introduction of rest particles in lattice gas automata [8] and to the permittivity stub that is used in the TLM method [18]. Actually node $\mathbf{r}_{2d+1}$ spatially coincides with node $\mathbf{r}$ and has only been introduced in order to describe the process of energy trapping at each node $\mathbf{r}$. As shown later, this process is necessary to handle inhomogeneous media. Since node $\mathbf{r}_{2d+1}$ is attached to node $\mathbf{r}$, $\mathbf{r}_{2d+1}$ will be next referred as $\mathbf{r}$ in order to simplify the notations inasmuch as there is no confusion between the processes that take place at each of both nodes.

Each node $\mathbf{r}$ of the lattice is a scatterer described by a matrix that instantaneously transforms the $2d+1$ incident currents $e_k(\mathbf{r},t)$, $k = 1, \dots 2d+1$ into $2d+1$ outgoing currents $s_k(\mathbf{r},t)$. Hence, the scattering process is described by

$$s_k(\mathbf{r},t) = \sum_{l=1}^{2d+1} d_{kl}(\mathbf{r}) e_l(\mathbf{r},t) \quad k = 1, \dots 2d+1 \qquad (2.1)$$

where the $d_{kl}(\mathbf{r})$ are the elements of the $(2d+1)\times(2d+1)$ scattering matrix D.

In the same way, node $\mathbf{r}_{2d+1}$ can be considered as a scatterer, which transforms the single incident current $e_{2d+2}(\mathbf{r}_{2d+1}, t)$ into the outgoing current $s_{2d+2}(\mathbf{r}_{2d+1}, t)$, which is sent back to node $\mathbf{r}$ at the next time step. Presently, $s_{2d+2}(\mathbf{r}_{2d+1}, t)$ can have any arbitrary value. For reasons to become clear soon, the scattering process at node $\mathbf{r}_{2d+1}$ is written as

$$s_{2d+2}(\mathbf{r},t) = -\mu_{2d+2}(\mathbf{r}) e_{2d+2}(\mathbf{r},t) + J(\mathbf{r},t) \qquad (2.2)$$

where $\mu_{2d+2}(\mathbf{r})$ and $J(\mathbf{r},t)$ are unknown. As mentioned before, $\mathbf{r}_{2d+1}$ is referred as $\mathbf{r}$ in (2.2). Later, without sources or losses, we shall see that (2.2) reads $s_{2d+2}(\mathbf{r}_{2d+1}, t) = \pm e_{2d+2}(\mathbf{r}_{2d+1}, t)$ thus corresponding to simple reflection at node $\mathbf{r}_{2d+1}$. The time evolution of the currents is summarized in Figure 2.

2.2 Definition of the fields

The field at node $\mathbf{r}$ and at time t is defined by a linear combination of the incident currents

$$\Psi(\mathbf{r},t) = \sum_{l=1}^{2d+1} \lambda_k(\mathbf{r}) e_k(\mathbf{r},t) \qquad (2.3)$$

where the $\lambda_k(\mathbf{r})$'s are real coefficients to be determined by the properties discussed below. This is the most general definition that takes linearity into account. At this stage, we do not associate any physical meaning to the field $\Psi(\mathbf{r},t)$. In particular, we allow for fields $\Psi(\mathbf{r},t)$ and $\Psi(\mathbf{r}',t)$ at two nodes $\mathbf{r}$ and $\mathbf{r}'$ to correspond to two different physical quantities. We will see later that $\Psi(\mathbf{r},t)$ can be any of the Cartesian components of the electric and magnetic fields. The location of these components will depend on the node $\mathbf{r}$.

2.3 Time evolution of the field

The most general explicit form of the discrete wave equation, which governs the time evolution of $\Psi(\mathbf{r},t)$ can be written:

$$\Psi(\mathbf{r}, t+\tau) = f\big(\Psi(\mathbf{r}',t'), \Psi(\mathbf{r}'',t''), \Psi(\mathbf{r}''',t'''), \dots\big) \qquad (2.4)$$

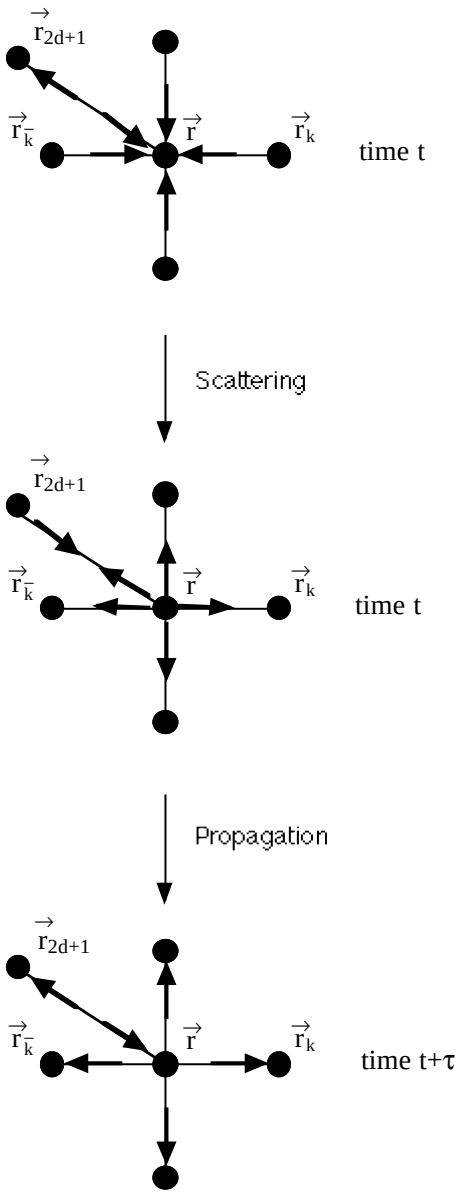

Fig. 2. Scattering and propagation of currents.

where the field at node $\mathbf{r}$ and at time $t+\tau$ is computed from known values of the field at specific nodes $\mathbf{r}', \mathbf{r}'', \ldots$ and at previous times t', t'', etc. By using (2.3), equation (2.4) becomes:

$$\sum_{k=1}^{2d+1} \lambda_k(\mathbf{r}) e_k(\mathbf{r}, t+\tau) = f\left(\sum_{k=1}^{2d+1} \lambda_k(\mathbf{r}') e_k(\mathbf{r}', t'), \sum_{k=1}^{2d+1} \lambda_k(\mathbf{r}'') e_k(\mathbf{r}'', t''), \sum_{k=1}^{2d+1} \lambda_k(\mathbf{r}''') e_k(\mathbf{r}''', t'''), \ldots \right). \tag{2.5}$$

However, if we use an arbitrary scattering matrix D, the propagation and scattering rules of the currents that are described in Section 2.1, do not lead to an equation like (2.5). It has been established in [6] that an evolution equation of the currents like (2.5) is possible if the elements of the scattering matrix D have the following form

$$d_{kl}(\mathbf{r}) = \rho_k(\mathbf{r})\lambda_l(\mathbf{r}) - \mu_k(\mathbf{r})\delta_{kl} \tag{2.6}$$

where the $\lambda_l(\mathbf{r})$ are the coefficients introduced in the definition of the field (2.3). $\rho_k(\mathbf{r})$ and $\mu_k(\mathbf{r})$ are new unknown coefficients and δ_{kl} is the Kronecker symbol. Moreover, $\mu_k(\mathbf{r})$ must satisfy the condition:

$$\forall \mathbf{r},\ \forall k = 1, \ldots 2d+1 \qquad \mu_k(\mathbf{r})\mu_{\overline{k}}(\mathbf{r}_k) = M \tag{2.7}$$

where the constant M is independent of the node position $\mathbf{r}$.

We do not reproduce here the derivation of (2.6) and (2.7), which is described in details in [6]. These two conditions are essential in the construction of the model and have been referred to as closure conditions in [6]. Without them, it would be impossible to obtain for $\Psi(\mathbf{r}, t)$ a closed equation like (2.4) where no current appears explicitly. Eventually, the current propagation and scattering rules, and (2.6, 2.7) lead to

$$\Psi(\mathbf{r}, t+\tau) + \Psi(\mathbf{r}, t-\tau) M \left[\sum_{k=1}^{2d+1} [\lambda_k(\mathbf{r})\rho_k(\mathbf{r})/\mu_k(\mathbf{r})] - 1 \right] = \sum_{k=1}^{2d} \lambda_k(\mathbf{r})\rho_{\overline{k}}(\mathbf{r}_k)\Psi(\mathbf{r}_k, t) + \lambda_{2d+1}(\mathbf{r})J(\mathbf{r}, t) \tag{2.8}$$

which is the time evolution equation of $\Psi(\mathbf{r}, t)$ we are looking for. To establish (2.8), we have also used the expression (2.2) of $s_{2d+2}(\mathbf{r}, t)$. Since equations (2.6, 2.7) lead to (2.8), they can be considered at this stage as a general but technical recipe, which transforms the time evolution of the currents in a finite difference scheme for the field $\Psi(\mathbf{r}, t)$. However, we show now that condition (2.6) also leads to a physical picture of the scattering process of the currents. For this purpose, one can check that (2.6) leads to the following form of the scattering equation (2.1)

$$s_k(\mathbf{r}, t) = \rho_k(\mathbf{r})\Psi(\mathbf{r}, t) - \mu_k(\mathbf{r})e_k(\mathbf{r}, t) \qquad k = 1, \ldots 2d+1. \tag{2.9}$$

The right hand side of equation (2.9) contains two terms: $\rho_k(\mathbf{r})\Psi(\mathbf{r}, t)$ and $\mu_k(\mathbf{r})e_k(\mathbf{r}, t)$. The first term states that the field $\Psi(\mathbf{r}, t)$ acts as a source at node $\mathbf{r}$ for all outgoing currents $s_k(\mathbf{r}, t)$ that are sent to the neighbor nodes at the next time step. Somehow, this term can be considered as a formulation of Huygens'principle. The second term states that the outgoing current $s_k(\mathbf{r}, t)$ keeps some memory of the incident current $e_k(\mathbf{r}, t)$ along the same bond k. This second term is essential to allow for propagation along some given direction in modifying the Huygens' term, which only describes isotropic reemission of wavelets.

As noted before, equation (2.2) is arbitrary since $\mu_{2d+2}(\mathbf{r})$ and $J(\mathbf{r}, t)$ are unknown. However, its expression is actually inspired from equation (2.9) for $s_k(\mathbf{r}, t)$, which is only valid for $k = 1, 2 \ldots 2d+1$. Hence, equation (2.2) is similar to (2.9) except that the role of the source is held

by the term $J(\mathbf{r},t)$ instead of the field $\Psi(\mathbf{r},t)$. We note also that $\mu_{2d+2}(\mathbf{r})$ is now connected to $\mu_{2d+1}(\mathbf{r})$ *via* (2.7).

The construction of the model goes further by introducing fundamental symmetries of the evolution of the currents. The first symmetry is time reversal, which implies that the scattering process is reversible when the directions of the current arrows are reversed. This yields the condition $D^{-1} = D$ for the scattering matrix. One easily obtains

$$\forall k = 1, \dots 2d+1 \qquad \mu_k(\mathbf{r}) = \eta(\mathbf{r}) \tag{2.10}$$

where $\eta(\mathbf{r}) = \pm 1$ and

$$\sum_{k=1}^{2d+1} \lambda_k(\mathbf{r})\rho_k(\mathbf{r}) = 2\eta(\mathbf{r}). \tag{2.11}$$

Equation (2.8) becomes

$$\Psi(\mathbf{r},t+\tau) + M\Psi(\mathbf{r},t-\tau) = \sum_{k=1}^{2d} \lambda_k(\mathbf{r})\rho_{\overline{k}}(\mathbf{r}_k)\Psi(\mathbf{r}_k,t) + \lambda_{2d+1}(\mathbf{r})J(\mathbf{r},t). \tag{2.12}$$

Note that (2.7) and (2.10) imply that $M = \pm 1$.

The next symmetry is reciprocity. Each matrix element d_{kl} of D describes one elementary scattering process, which is transmission, reflection or scattering. It couples the two channels (bonds) k and l. Reciprocity means that the scattering process from k to l and the reciprocal process from l to k have the same amplitude. In other words, $\forall k, l = 1, \dots 2d+1$, $d_{lk} = d_{kl}$. Thus, the matrix D is symmetrical. Note that the properties $D^{-1} = D$ and $D = D^t$ imply that D is orthogonal. This important property implies that the time evolution of the currents is unconditionally stable.

One easily obtains

$$\forall k = 1, \dots 2d+1 \qquad \rho_k(\mathbf{r}) = 2\eta(\mathbf{r})\lambda_k(\mathbf{r})/\Lambda(\mathbf{r}) \tag{2.13}$$

$$d_{kl}(\mathbf{r}) = \eta(\mathbf{r})\big[2\lambda_k(\mathbf{r})\lambda_l(\mathbf{r})/\Lambda(\mathbf{r}) - \delta_{kl}\big] \tag{2.14}$$

where $\Lambda(\mathbf{r}) = \sum_{k=1}^{2d+1} \lambda_k^2(\mathbf{r})$. The only parameters that remain unknown are the $\lambda_k(\mathbf{r})$'s.

The propagation equation (2.12) now reads

$$\Psi(\mathbf{r},t+\tau) + M\Psi(\mathbf{r},t-\tau) = 2M\eta(\mathbf{r}) \sum_{k=1}^{2d} \big[\lambda_k(\mathbf{r})\lambda_{\overline{k}}(\mathbf{r}_k)/\Lambda(\mathbf{r}_k)\big]\Psi(\mathbf{r}_k,t) + \lambda_{2d+1}(\mathbf{r})J(\mathbf{r},t). \tag{2.15}$$

At this stage, it is convenient to replace the definition (2.3) of the field by

$$\Psi(\mathbf{r},t) = (1/\Lambda(\mathbf{r})) \sum_{k=1}^{2d+1} \lambda_k(\mathbf{r})e_k(\mathbf{r},t) \tag{2.16}$$

so that (2.15) becomes

$$\Psi(\mathbf{r},t+\tau) + M\Psi(\mathbf{r},t-\tau) = (2M\eta(\mathbf{r})/\Lambda(\mathbf{r})) \times \sum_{k=1}^{2d} \lambda_k(\mathbf{r})\lambda_{\overline{k}}(\mathbf{r}_k)\Psi(\mathbf{r}_k,t) + \lambda_{2d+1}(\mathbf{r})J(\mathbf{r},t)/\Lambda(\mathbf{r}). \tag{2.17}$$

With this new definition of the field, the scattering equation (2.9) becomes

$$s_k(\mathbf{r},t) = \eta(\mathbf{r})[2\lambda_k(\mathbf{r})\Psi(\mathbf{r},t) - e_k(\mathbf{r},t)] \tag{2.18}$$

a result that will be useful in Section 3. To establish (2.18), we have used (2.10) and (2.13). In the same way, equation (2.2) reads

$$s_{2d+2}(\mathbf{r},t) = J(\mathbf{r},t) - M\eta(\mathbf{r})e_{2d+2}(\mathbf{r},t) \tag{2.19}$$

where we have used $\mu_{2d+2}(\mathbf{r}) = M\eta(\mathbf{r})$, which results from (2.7) and (2.10). As noted before, if $J(\mathbf{r},t) = 0$, then $s_{2d+2}(\mathbf{r},t) = \pm e_{2d+2}(\mathbf{r},t)$ since $M\eta(\mathbf{r}) = \pm 1$.

This section achieves the general construction of a wave automaton from first principles, namely the equivalent of a discrete Huygens' principle, which governs the dynamics of the currents, and fundamental symmetry properties. However, at this stage of the model, the values of the coefficients M and $\lambda_k(\mathbf{r})$ are still unknown. The next section is devoted to the derivation of the Maxwell's equations from appropriate choices of these parameters.

3 Derivation of the Maxwell's equations

In this section, we set $J(\mathbf{r},t) = 0$ for convenience. The term $J(\mathbf{r},t)$ can be reintroduced later as a source term for Maxwell's equations. We shall also consider a homogeneous system. At first sight, this must imply that the coefficients $\lambda_k(\mathbf{r})$ do not depend on the node position $\mathbf{r}$. Actually, we shall see that two neighbor nodes are not equivalent so that the coefficients $\lambda_k(\mathbf{r})$ do depend on the node position. The definition of a homogeneous system will be made more precise during the development of this section. First, we start by discussing the value of the parameter M.

3.1 Choice of the parameter M

The parameter M has been introduced in the closure condition (2.7) as a constant independent of the node position $\mathbf{r}$. Due to the time-reversal symmetry result (2.10), equation (2.7) reads

$$M = \eta(\mathbf{r})\eta(\mathbf{r}_k). \tag{3.1}$$

As noted before, this implies that $M = \pm 1$. Since M has the same value for all nodes $\mathbf{r}$ of the lattice, two separate cases must be considered: $M = +1$ and $M = -1$. If $M = +1$, the left-hand side of (2.17) indicates that $\Psi(\mathbf{r},t)$

is bound to obey a second order time derivative equation. Moreover, $\forall \mathbf{r}$, $\forall \mathbf{r}_k$, $\eta(\mathbf{r}) = \eta(\mathbf{r}_k) = \eta$ where $\eta = \pm 1$ does not depend on node $\mathbf{r}$. This case has been considered in the previous versions of the wave automaton and leads to the time-dependent scalar wave equation [6,14]. Hence, we shall consider the second case $M = -1$ in the rest of this paper. Then, $\Psi(\mathbf{r}, t)$ obeys a first order time derivative equation according to (2.17). Moreover, (3.1) implies that $\forall \mathbf{r}$, $\forall k$, $\eta(\mathbf{r}_k) = -\eta(\mathbf{r})$. In other words, the lattice is decomposed in two intermingled sub-lattices according to a checkerboard pattern, one sub-lattice where $\eta(\mathbf{r}) = +1$ and one sub-lattice where $\eta(\mathbf{r}) = -1$. This property indicates that the field at node $\mathbf{r}$ will have a physical content different from the fields at its neighbor nodes $\mathbf{r}_k$.

A clue as to the physical content of $\Psi(\mathbf{r}, t)$ is provided by time-reversal symmetry. According to (2.16), $\Psi(\mathbf{r}, t)$ is defined as

$$\Psi(\mathbf{r}, t) = (1/\Lambda(\mathbf{r})) \sum_{k=1}^{2d+1} \lambda_k(\mathbf{r}) e_k(\mathbf{r}, t). \tag{3.2}$$

Time reversal is achieved by reversing the current arrows. Hence, the time-reversed field $\Psi^{\mathrm{tr}}(\mathbf{r}, t)$ is defined as a function of the outgoing currents $s_k(\mathbf{r}, t)$

$$\Psi^{\mathrm{tr}}(\mathbf{r}, t) = (1/\Lambda(\mathbf{r})) \sum_{k=1}^{2d+1} \lambda_k(\mathbf{r}) s_k(\mathbf{r}, t). \tag{3.3}$$

Using (2.18), one easily finds

$$\Psi^{\mathrm{tr}}(\mathbf{r}, t) = \eta(\mathbf{r}) \Psi(\mathbf{r}, t). \tag{3.4}$$

Equation (3.4) means that $\Psi(\mathbf{r}, t)$ is invariant under time-reversal symmetry over the sub-lattice $\eta(\mathbf{r}) = +1$ and changes sign over the sub-lattice $\eta(\mathbf{r}) = -1$. Hence, anticipating the Maxwell's equations, the fields $\Psi(\mathbf{r}, t)$ over the sub-lattices $\eta(\mathbf{r}) = +1$ and $\eta(\mathbf{r}) = -1$ will correspond to the electric and magnetic fields respectively. From now, we introduce the following notation for these two kinds of fields: ${}^{+}\Psi(\mathbf{r}, t)$ and ${}^{-}\Psi(\mathbf{r}, t)$.

3.2 Transformation of the parameters $\lambda_k(\mathbf{r})$ under local inversion

In this section, we first rewrite the wave equations for the fields ${}^{+}\Psi(\mathbf{r}, t)$ and ${}^{-}\Psi(\mathbf{r}, t)$. We show that these equations are first order spatial derivative equations like the Maxwell's equations if the $\lambda_k(\mathbf{r})$'s behave properly under local inversion. Let us first rewrite (2.17) with $M = -1$ (and $J(\mathbf{r}, t) = 0$)

$$\begin{aligned} {}^{\eta}\Psi(\mathbf{r}, t+\tau) - {}^{\eta}\Psi(\mathbf{r}, t-\tau) = -(2\eta(\mathbf{r})/\Lambda(\mathbf{r})) \\ \times \sum_{k=1}^{2d} \lambda_k(\mathbf{r}) \lambda_{\overline{k}}(\mathbf{r}_k) {}^{-\eta}\Psi(\mathbf{r}_k, t) \end{aligned} \tag{3.5}$$

where

$$\eta \equiv \eta(\mathbf{r}) = -\eta(\mathbf{r}_k) = \pm 1. \tag{3.6}$$

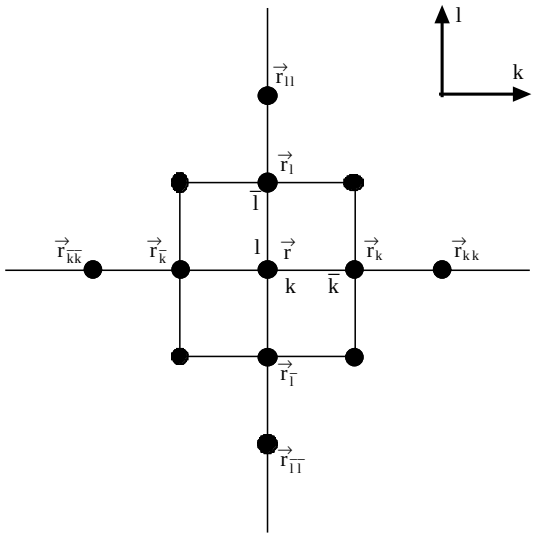

Fig. 3. Notation for central node $\mathbf{r}$ and its neighbors. Note that with this notation, $\mathbf{r}_{k\overline{k}} \equiv \mathbf{r}$.

By assembling the terms k and $\overline{k}$ along each direction $[k, \overline{k}]$, (3.5) can be written

$$\begin{aligned} {}^{\eta}\Psi(\mathbf{r}, t+\tau) - {}^{\eta}\Psi(\mathbf{r}, t-\tau) = -(2\eta(\mathbf{r})/\Lambda(\mathbf{r})) \sum_{k=1}^{d} (1/2) \\ \times \left\{ \left[\lambda_k(\mathbf{r}) \lambda_{\overline{k}}(\mathbf{r}_k) - \lambda_{\overline{k}}(\mathbf{r}) \lambda_k(\mathbf{r}_{\overline{k}}) \right] \left[{}^{-\eta}\Psi(\mathbf{r}_k, t) - {}^{-\eta}\Psi(\mathbf{r}_{\overline{k}}, t) \right] \right. \\ \left. + \left[\lambda_k(\mathbf{r}) \lambda_{\overline{k}}(\mathbf{r}_k) + \lambda_{\overline{k}}(\mathbf{r}) \lambda_k(\mathbf{r}_{\overline{k}}) \right] \left[{}^{-\eta}\Psi(\mathbf{r}_k, t) + {}^{-\eta}\Psi(\mathbf{r}_{\overline{k}}, t) \right] \right\} . \end{aligned} \tag{3.7}$$

In (3.7), the summation is made over the d directions $[k, \overline{k}]$ instead of the $2d$ bonds as in (3.5). As stated before, we consider a homogeneous system. Since the lattice is made of two intermingled sub-lattices $\eta = +1$ and $\eta = -1$, this implies that each node $\mathbf{r}$ is not equivalent to its first neighbors $\mathbf{r}_k$ but to its second neighbors $\mathbf{r}_{kk}$ (Fig. 3). In the same way, node $\mathbf{r}_{\overline{k}}$ becomes equivalent to node $\mathbf{r}_k$. Hence, we can write

$$\lambda_k(\mathbf{r}_{\overline{k}}) = \lambda_k(\mathbf{r}_k). \tag{3.8}$$

To go further, we remind the reader that in previous versions of the wave automaton devoted to scalar wave propagation, the coefficients $\lambda_k(\mathbf{r})$'s have been determined by assuming additional symmetries such as isotropy [6] or local inversion symmetry [14] of the scattering process. The same symmetry arguments can be used here. In this section, we shall start by assuming local inversion symmetry. The part played by isotropy will be discussed in the next sections.

It is well known that the components of the electric field change sign under inversion of the coordinate axis. In contrast, the components of the magnetic field do not change sign. In other words, the electric field is a vector field and the magnetic field is a pseudovector field. Hence, it will not come as a surprise that the coefficients $\lambda_k(\mathbf{r})$

will also exhibit different behaviors under local inversion. Actually, local inversion symmetry can be defined in different ways. Let us start by writing it as

$$\forall k, \quad \lambda_{\overline{k}}(\mathbf{r}) = \lambda_k(\mathbf{r}) \tag{3.9}$$

Hence, using (3.8) and (3.9), (3.7) becomes

$$^{\eta}\Psi(\mathbf{r}, t+\tau) - {}^{\eta}\Psi(\mathbf{r}, t-\tau) = -(4\eta(\mathbf{r})/\Lambda(\mathbf{r})) \times \sum_{k=1}^{d} \lambda_k(\mathbf{r})\lambda_{\overline{k}}(\mathbf{r}_k) \left[{}^{-\eta}\Psi(\mathbf{r}_k, t) + {}^{-\eta}\Psi(\mathbf{r}_{\overline{k}}, t)\right]/2. \tag{3.10}$$

The quantity $[{}^{-\eta}\Psi(\mathbf{r}_k, t) + {}^{-\eta}\Psi(\mathbf{r}_{\overline{k}}, t)]/2$ that appears in (3.10) can be considered as the average field ${}^{-\eta}\Psi_{av}(\mathbf{r}, t)$. Hence, (3.10) is the discrete counterpart of the following continuum equation

$$\partial^{\eta}\Psi/\partial t = -(2\eta(\mathbf{r})/\tau\Lambda(\mathbf{r})) \sum_{k=1}^{d} \lambda_k(\mathbf{r})\lambda_{\overline{k}}(\mathbf{r}_k) {}^{-\eta}\Psi(\mathbf{r}, t). \tag{3.11}$$

Note that if we had chosen to write local inversion symmetry as $\forall k$, $\lambda_{\overline{k}}(\mathbf{r}) = -\lambda_k(\mathbf{r})$, we would also have obtained (3.11). Let us compare with Maxwell's equations, which read in Cartesian coordinates

$$\varepsilon_0\varepsilon_i\, \partial E_i/\partial t = \partial H_k/\partial x_j - \partial H_j/\partial x_k \tag{3.12a}$$

$$\mu_0\mu_i\, \partial H_i/\partial t = \partial E_j/\partial x_k - \partial E_k/\partial x_j \tag{3.12b}$$

where i, j, k is any cyclic permutation of x, y, z. In (3.12a) and (3.12b), $\varepsilon_0\varepsilon_i$ and $\mu_0\mu_i$ are the diagonal elements of the permittivity and permeability tensors respectively. It is obvious that (3.11) is not a first order spatial derivative equation like Maxwell's equations (3.12). At first sight, this result is disappointing since before stating local inversion symmetry, the original equation (3.7) included the discrete first order spatial derivative term ${}^{-\eta}\Psi(\mathbf{r}_k, t) - {}^{-\eta}\Psi(\mathbf{r}_{\overline{k}}, t)$. The problem we are facing comes from the definition (3.9) of local inversion symmetry. Actually, there is a third way to write local inversion symmetry, namely

$$\forall k, \quad \lambda_{\overline{k}}(\mathbf{r}) = \eta(\mathbf{r})\lambda_k(\mathbf{r}) \tag{3.13}$$

instead of (3.9). In this case, (3.7) becomes

$$^{\eta}\Psi(\mathbf{r}, t+\tau) - {}^{\eta}\Psi(\mathbf{r}, t-\tau) = -(2\eta(\mathbf{r})/\Lambda(\mathbf{r})) \times \sum_{k=1}^{d} \lambda_k(\mathbf{r})\lambda_{\overline{k}}(\mathbf{r}_k) \left[{}^{-\eta}\Psi(\mathbf{r}_k, t) - {}^{-\eta}\Psi(\mathbf{r}_{\overline{k}}, t)\right]. \tag{3.14}$$

The term $[{}^{-\eta}\Psi(\mathbf{r}_k, t) - {}^{-\eta}\Psi(\mathbf{r}_{\overline{k}}, t)]/2$ in (3.14) is the discrete spatial derivative of the field ${}^{-\eta}\Psi(\mathbf{r}, t)$ along the direction $[k, \overline{k}]$. Hence, (3.14) has the same form as Maxwell's equations (3.12). Therefore, we shall adopt (3.13) as the definition of local inversion symmetry. This choice can give the impression that we need to know ahead of time what the Maxwell's equations look like so that to be able to use the appropriate symmetries and eventually arrive at these equations. This impression is true but the point is that the general rules, which govern the wave automaton, as described in Section 2 of this paper contain virtually many different wave equations. Only appropriate choices of the underlying symmetries will restrict this choice until we obtain the wave equation we are looking for. Hence, the question is among all the possible choices, is there one that leads to the Maxwell's equations as other choices have already led to scalar wave equations [6]. This is the way we have proceeded in adopting (3.13). Obviously, the choice of a given symmetry should reflect a general property of the wave equation under consideration as we show now for local inversion symmetry as given by (3.13).

Note first, that we also obtain (3.14) if instead of (3.13), we define local inversion symmetry by $\forall \mathbf{r}$, $\lambda_{\overline{k}}(\mathbf{r}) = -\eta(\mathbf{r})\lambda_k(\mathbf{r})$. It can be shown that the choice between these two possibilities is a matter of convention and we shall only consider (3.13). Let us rewrite (3.13) as

$$\lambda_k^{\mathrm{inv}}(\mathbf{r}) = \eta(\mathbf{r})\lambda_{\overline{k}}(\mathbf{r}). \tag{3.15}$$

Under inversion of spatial coordinates, we can also write

$$e_k^{\mathrm{inv}}(\mathbf{r}, t) = -e_{\overline{k}}(\mathbf{r}, t). \tag{3.16}$$

The current indices k and $\overline{k}$ are exchanged in this transformation and the current takes the opposite sign since the directions of the axes are reversed. Hence, the field ${}^{\eta}\Psi(\mathbf{r}, t) = (1/\Lambda(\mathbf{r})) \sum_{k=1}^{2d+1} \lambda_k(\mathbf{r}) e_k(\mathbf{r}, t)$ becomes

$$\begin{aligned} {}^{\eta}\Psi^{\mathrm{inv}}(\mathbf{r}, t) &= (1/\Lambda^{\mathrm{inv}}(\mathbf{r})) \sum_{k=1}^{2d+1} \lambda_k^{\mathrm{inv}}(\mathbf{r}) e_k^{\mathrm{inv}}(\mathbf{r}, t) \\ &= -\eta(\mathbf{r})(1/\Lambda(\mathbf{r})) \sum_{k=1}^{2d+1} \lambda_{\overline{k}}(\mathbf{r}) e_{\overline{k}}(\mathbf{r}, t) \end{aligned}$$

where $\Lambda^{\mathrm{inv}}(\mathbf{r}) = \sum_{k=1}^{2d+1} [\lambda_k^{\mathrm{inv}}(\mathbf{r})]^2 = \Lambda(\mathbf{r})$.

Hence

$$^{\eta}\Psi^{\mathrm{inv}}(\mathbf{r}, t) = -\eta(\mathbf{r})\, {}^{\eta}\Psi(\mathbf{r}, t). \tag{3.17}$$

Equation (3.17) shows the fields ${}^{+}\Psi(\mathbf{r}, t)$ and ${}^{-}\Psi(\mathbf{r}, t)$ behave in opposite ways

$$^{+}\Psi^{\mathrm{inv}}(\mathbf{r}, t) = -{}^{+}\Psi(\mathbf{r}, t) \tag{3.18a}$$

$$^{-}\Psi^{\mathrm{inv}}(\mathbf{r}, t) = +{}^{-}\Psi(\mathbf{r}, t). \tag{3.18b}$$

This is the expected behavior of the components of the electric and magnetic fields in the Maxwell's equations under local inversion symmetry. Let us recapitulate the main result of this section. If local inversion of the $\lambda_k(\mathbf{r})$'s is defined in such a way that the wave equation (3.5) becomes a first order spatial equation like the Maxwell's equations, then the fields ${}^{+}\Psi(\mathbf{r}, t)$ and ${}^{-}\Psi(\mathbf{r}, t)$ automatically behave under inversion of the coordinates as the components

of the electric and magnetic fields respectively. We could have done it the other way. If we impose that ${}^{+}\Psi(\mathbf{r},t)$ and ${}^{-}\Psi(\mathbf{r},t)$ behave as the components of a vector and of a pseudovector respectively, then equation (3.5) transforms itself into (3.14).

At this stage, we have obtained equation (3.14) for ${}^{+}\Psi(\mathbf{r},t)$ and ${}^{-}\Psi(\mathbf{r},t)$, which have the same time and spatial dependence as Maxwell's equations. To complete the construction, we must define the physical contents of ${}^{+}\Psi(\mathbf{r},t)$ and ${}^{-}\Psi(\mathbf{r},t)$, and establish the correspondence between the values of the $\lambda_k(\mathbf{r})$'s and the elements of permittivity and permeability tensors.

3.3 The vector fields ${}^{+}\boldsymbol{\Psi}(\mathbf{r},t)$ and ${}^{-}\boldsymbol{\Psi}(\mathbf{r},t)$

Let us rewrite (3.14) for the fields ${}^{+}\Psi(\mathbf{r},t)$ and ${}^{-}\Psi(\mathbf{r},t)$ by taking into account the results of the previous section. Restricting ourselves to the three dimensional physical space $d=3$ and a being the lattice constant, equation (3.14) becomes

$$\begin{aligned}\left[{}^{+}\Psi(\mathbf{r},t+\tau)\right. &\left.-{}^{+}\Psi(\mathbf{r},t-\tau)\right]/2\tau = -(2c_0/{}^{+}\Lambda(\mathbf{r}))\\ &\times\left\{{}^{+}t_x(\mathbf{r})\left[{}^{-}\Psi(\mathbf{r}_x,t)-{}^{-}\Psi(\mathbf{r}_{\overline{x}},t)\right]\right.\\ &+{}^{+}t_y(\mathbf{r})\left[{}^{-}\Psi(\mathbf{r}_y,t)-{}^{-}\Psi(\mathbf{r}_{\overline{y}},t)\right]\\ &\left.+{}^{+}t_z(\mathbf{r})\left[{}^{-}\Psi(\mathbf{r}_z,t)-{}^{-}\Psi(\mathbf{r}_{\overline{z}},t)\right]\right\}/2a\end{aligned}\tag{3.19a}$$

$$\begin{aligned}\left[{}^{-}\Psi(\mathbf{r},t+\tau)\right. &\left.-{}^{-}\Psi(\mathbf{r},t-\tau)\right]/2\tau = +(2c_0/{}^{-}\Lambda(\mathbf{r}))\\ &\times\left\{{}^{-}t_x(\mathbf{r})\left[{}^{+}\Psi(\mathbf{r}_x,t)-{}^{+}\Psi(\mathbf{r}_{\overline{x}},t)\right]\right.\\ &+{}^{-}t_y(\mathbf{r})\left[{}^{+}\Psi(\mathbf{r}_y,t)-{}^{+}\Psi(\mathbf{r}_{\overline{y}},t)\right]\\ &\left.+{}^{-}t_z(\mathbf{r})\left[{}^{+}\Psi(\mathbf{r}_z,t)-{}^{+}\Psi(\mathbf{r}_{\overline{z}},t)\right]\right\}/2a\end{aligned}\tag{3.19b}$$

where $c_0 = a/\tau$ is the current velocity. In (3.19a) and (3.19b), we have generalized the use of the superscripts + and − to emphasize that parameters like $\lambda_k(\mathbf{r})$ or $\Lambda(\mathbf{r})$ are defined over the two distinct sub-lattices $\eta=+1$ and $\eta=-1$. In particular, we have introduced the following condensed notation

$${}^{\eta}t_k(\mathbf{r}) = {}^{\eta}\lambda_k(\mathbf{r})^{-\eta}\lambda_{\overline{k}}(\mathbf{r}).\tag{3.20}$$

Equations (3.19a) and (3.19b) are the discrete versions of the following continuum equations

$$\begin{aligned}\partial^{+}\Psi/\partial\tau &= -(2c_0/{}^{+}\Lambda)\\ &\times\left\{{}^{+}t_x\partial^{-}\Psi/\partial x+{}^{+}t_y\partial^{-}\Psi/\partial y+{}^{+}t_z\partial^{-}\Psi/\partial z\right\}\end{aligned}\tag{3.21a}$$

$$\begin{aligned}\partial^{-}\Psi/\partial\tau &= +(2c_0/{}^{-}\Lambda)\\ &\times\left\{{}^{-}t_x\partial^{+}\Psi/\partial x+{}^{-}t_y\partial^{+}\Psi/\partial y+{}^{-}t_z\partial^{+}\Psi/\partial z\right\}.\end{aligned}\tag{3.21b}$$

Comparison with (3.12a) and (3.12b) reveals that additional choices must be made for the wave automaton to reduce to Maxwell's equations. In particular, we must stipulate that the fields we deal with are vector fields, a statement that has not yet be done in our construction until now. At first sight, this seems to contradict the fact that in (3.21a) and (3.21b), ${}^{+}\Psi(\mathbf{r},t)$ and ${}^{-}\Psi(\mathbf{r},t)$ are two scalar and pseudoscalar fields respectively. Actually, ${}^{+}\Psi(\mathbf{r},t)$ and ${}^{-}\Psi(\mathbf{r},t)$ are not vector fields but can be considered as the Cartesian components ${}^{+}\Psi_x(\mathbf{r},t)$, ${}^{+}\Psi_y(\mathbf{r},t)$, ${}^{+}\Psi_z(\mathbf{r},t)$ and ${}^{-}\Psi_x(\mathbf{r},t)$, ${}^{-}\Psi_y(\mathbf{r},t)$, ${}^{-}\Psi_z(\mathbf{r},t)$ of appropriate vector fields ${}^{+}\boldsymbol{\Psi}(\mathbf{r},t)$ and ${}^{-}\boldsymbol{\Psi}(\mathbf{r},t)$. Therefore, let us rewrite (3.19a) and (3.19b) by assuming that ${}^{+}\Psi(\mathbf{r},t)$ and ${}^{-}\Psi(\mathbf{r},t)$ are such Cartesian components

$$\begin{aligned}\left[{}^{+}\Psi_i(\mathbf{r},t+\tau)\right. &\left.-{}^{+}\Psi_i(\mathbf{r},t-\tau)\right]/2\tau = -(2c_0/{}^{+}\Lambda(\mathbf{r}))\\ &\times\left\{{}^{+}t_x(\mathbf{r})\left[{}^{-}\Psi_k(\mathbf{r}_x,t)-{}^{-}\Psi_k(\mathbf{r}_{\overline{x}},t)\right]\right.\\ &+{}^{+}t_y(\mathbf{r})\left[{}^{-}\Psi_l(\mathbf{r}_y,t)-{}^{-}\Psi_l(\mathbf{r}_{\overline{y}},t)\right]\\ &\left.+{}^{+}t_z(\mathbf{r})\left[{}^{-}\Psi_m(\mathbf{r}_z,t)-{}^{-}\Psi_m(\mathbf{r}_{\overline{z}},t)\right]\right\}/2a\end{aligned}\tag{3.22a}$$

$$\begin{aligned}\left[{}^{-}\Psi_j(\mathbf{r},t+\tau)\right. &\left.-{}^{-}\Psi_j(\mathbf{r},t-\tau)\right]/2\tau = +(2c_0/{}^{-}\Lambda(\mathbf{r}))\\ &\times\left\{{}^{-}t_x(\mathbf{r})\left[{}^{+}\Psi_n(\mathbf{r}_x,t)-{}^{+}\Psi_n(\mathbf{r}_{\overline{x}},t)\right]\right.\\ &+{}^{-}t_y(\mathbf{r})\left[{}^{+}\Psi_o(\mathbf{r}_y,t)-{}^{+}\Psi_o(\mathbf{r}_{\overline{y}},t)\right]\\ &\left.+{}^{-}t_z(\mathbf{r})\left[{}^{+}\Psi_p(\mathbf{r}_z,t)-{}^{+}\Psi_p(\mathbf{r}_{\overline{z}},t)\right]\right\}/2a\end{aligned}\tag{3.22b}$$

where the indices i,j,k,l,m,n,o,p can be any of the Cartesian coordinates x,y,z. Note first that the different components ${}^{+}\Psi_x(\mathbf{r},t)$, ${}^{+}\Psi_y(\mathbf{r},t)$, ${}^{+}\Psi_z(\mathbf{r},t)$ cannot exist at the same nodes of the sub-lattice $\eta(\mathbf{r})=+1$. Otherwise, we should be obliged to modify our construction to introduce several currents propagating between nodes, one for each component defined at the same node. In the same way, ${}^{-}\Psi_x(\mathbf{r},t)$, ${}^{-}\Psi_y(\mathbf{r},t)$, ${}^{-}\Psi_z(\mathbf{r},t)$ are not defined at the same nodes of the sub-lattice $\eta(\mathbf{r})=-1$. Hence, our next step is to find the node location of the different components ${}^{+}\Psi_i(\mathbf{r},t)$ and ${}^{-}\Psi_j(\mathbf{r},t)$. This task will be facilitated by noticing that (3.22a) and (3.22b) are very close to Maxwell's equations (3.12) that we write below in discrete form

$$\begin{aligned}&\left[E_i(\mathbf{r},t+\tau)-E_i(\mathbf{r},t-\tau)\right]/2\tau = (1/\varepsilon_0\varepsilon_i)\\ &\times\left\{\left[H_k(\mathbf{r}_j,t)-H_k(\mathbf{r}_{\overline{j}},t)\right]-\left[H_j(\mathbf{r}_k,t)-H_j(\mathbf{r}_{\overline{k}},t)\right]\right\}/2a\end{aligned}\tag{3.23a}$$

$$\begin{aligned}&\left[H_i(\mathbf{r},t+\tau)-H_i(\mathbf{r},t-\tau)\right]/2\tau = (1/\mu_0\mu_i)\\ &\times\left\{\left[E_j(\mathbf{r}_k,t)-E_j(\mathbf{r}_{\overline{k}},t)\right]-\left[E_k(\mathbf{r}_j,t)-E_k(\mathbf{r}_{\overline{j}},t)\right]\right\}/2a\end{aligned}\tag{3.23b}$$

where the indices i,j,k are any circular permutation of x,y,z.

Actually, equations (3.22) are identical to equations (3.23) if the parameters $\pm 2c_0{}^{\eta}t_k(\mathbf{r})/{}^{\eta}\Lambda(\mathbf{r})$ in (3.22) are identified with the terms $\pm 1/\varepsilon_0\varepsilon_i$ and $\pm 1/\mu_0\mu_i$ in (3.23). We perform this task in the next section.

$$
\begin{aligned}
{}^{+}\Psi[(2l+1)a, 2ma, (2n+1)a] &\equiv E_x[(2l+1)a, 2ma, (2n+1)a] \\
{}^{+}\Psi[2la, (2m+1)a, (2n+1)a] &\equiv E_y[2la, (2m+1)a, (2n+1)a] \\
{}^{+}\Psi[2la, 2ma, 2na] &\equiv E_z[2la, 2ma, 2na] \\
{}^{-}\Psi[2la, (2m+1)a, 2na] &\equiv H_x[2la, (2m+1)a, 2na] \\
{}^{-}\Psi[(2l+1)a, 2ma, 2na] &\equiv H_y[(2l+1)a, 2ma, 2na] \\
{}^{-}\Psi[(2l+1)a, (2m+1)a, (2n+1)a] &\equiv H_z[(2l+1)a, (2m+1)a, (2n+1)a]. \qquad (3.24)
\end{aligned}
$$

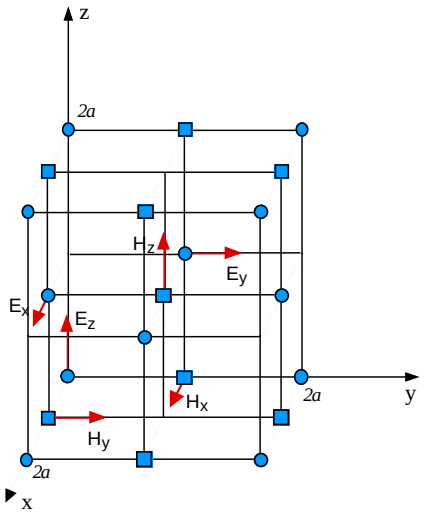

Fig. 4. Yee cell geometry. The lattice period is $2a$ where a is the distance between two neighbor nodes.

3.4 Identification of the wave automaton with Maxwell's equations

The discrete equations (3.23) are commonly used in the Finite Difference Time Domain Method (FDTD) [19,20] and are associated to the Yee cell geometry [16], which is displayed in Figure 4. In this geometry, the electric field and magnetic field components are located at the nodes indicated in the figure. If the positions of the different components are given in terms of the unit step a along each direction x, y and z, and assuming for instance that the component E_z is located at the origin, the different components can be written as $E_x[(2l+1)a, 2ma, (2n+1)a]$, $E_y[2la, (2m+1)a, (2n+1)a]$, $E_z(2la, 2ma, 2na)$, $H_x[2la, (2m+1)a, 2na]$, $H_y[(2l+1)a, 2ma, 2na]$ and $H_z[(2l+1)a, (2m+1)a, (2n+1)a]$ where l, m and n are arbitrary integers.

Hence, comparison of (3.22) and (3.23) yields

see equation (3.24) above.

In the same way, the parameters $\pm 2c_0{}^{\eta}t_k(\mathbf{r})/{}^{\eta}\Lambda(\mathbf{r})$ in (3.22) have to be identified with the terms $\pm 1/\varepsilon_0\varepsilon_i$ and $\pm 1/\mu_0\mu_i$ in (3.23). Although straightforward, this task is rather lengthy and is described in the Appendix. This results in the following set of equations

$$
\begin{aligned}
{}^{+}\Lambda[(2l+1)a,&2ma, (2n+1)a]/\varepsilon_0\varepsilon_x \\
&= {}^{+}\Lambda[2la, (2m+1)a, (2n+1)a]/\varepsilon_0\varepsilon_y \\
&= {}^{+}\Lambda[2la, 2ma, 2na]/\varepsilon_0\varepsilon_z \\
&= {}^{-}\Lambda[2la, (2m+1)a, 2na]/\mu_0\mu_x \qquad (3.25) \\
&= {}^{-}\Lambda[(2l+1)a, 2ma, 2na]/\mu_0\mu_y \\
&= {}^{-}\Lambda[(2l+1)a, (2m+1)a, (2n+1)a]/\mu_0\mu_z
\end{aligned}
$$

which show that the elements $\varepsilon_0\varepsilon_i$ and $\mu_0\mu_j$ of the permittivity and permeability tensors respectively are controlled by the values of the parameters ${}^{\eta}\Lambda(\mathbf{r}) = \sum_{k=1}^{7} {}^{\eta}\lambda_k^2(\mathbf{r})$. At this stage the λ_k's are still unknown. To proceed further, we shall first consider the case of vacuum, *i.e.* $\varepsilon_i = 1$ and $\mu_j = 1$, before discussing the general case.

3.5 Determination of the parameters $\lambda_k(\mathbf{r})$

3.5.1 Case of vacuum

Since $\varepsilon_i = 1$ and $\mu_j = 1$, from (3.25) we immediately obtain

$$
\begin{aligned}
&{}^{+}\Lambda[(2l+1)a, 2ma, (2n+1)a] = \\
&{}^{+}\Lambda[2la, (2m+1)a, (2n+1)a] = {}^{+}\Lambda[2la, 2ma, 2na] = {}^{+}\Lambda_0 \qquad (3.26)
\end{aligned}
$$

and

$$
\begin{aligned}
{}^{-}\Lambda[2la, (2m+1)a, 2na] = {}^{-}\Lambda[(2l+1)a, 2ma, 2na] = \\
{}^{-}\Lambda[(2l+1)a, (2m+1)a, (2n+1)a] = {}^{-}\Lambda_0 \qquad (3.27)
\end{aligned}
$$

where the unique values of ${}^{+}\Lambda(\mathbf{r})$ and ${}^{-}\Lambda(\mathbf{r})$ are referred to as ${}^{+}\Lambda_0$ and ${}^{-}\Lambda_0$ respectively. Hence, (3.25) reads

$$
{}^{+}\Lambda_0/\varepsilon_0 = {}^{-}\Lambda_0/\mu_0. \qquad (3.28)
$$

As mentioned in Section 2.1, the role of the currents $e_7(\mathbf{r})$ and $s_7(\mathbf{r})$ that propagate over the bond $2d+1=7$ is to trap a fraction of the energy at node $\mathbf{r}$ at each time step. We also know that in the scalar versions of the wave automaton [6,14] the value of the parameter $\lambda_7(\mathbf{r})$ controls the velocity of the wave. This will be also the case here. In particular, the velocity of the wave is maximum when

the trapping effect is set to zero. Hence, for vacuum we must set $\lambda_7(\mathbf{r})$ to zero. Therefore, ${}^{\eta}\Lambda_0$ is given by

$$ {}^{\eta}\Lambda_0 \equiv \sum_{k=1}^{7} {}^{\eta}\lambda_k^2 = \sum_{k=1}^{6} {}^{\eta}\lambda_k^2 = \sum_{k'=1}^{4} {}^{\eta}\lambda_{k'}^2. \tag{3.29} $$

In (3.29), the first equality is the definition of ${}^{\eta}\Lambda_0$. The second equality states that ${}^{\eta}\lambda_7(\mathbf{r}) = 0$. The third equality specifies that there are only four incident propagating currents at each node of the Yee scheme (Eq. (A.19) in the Appendix). In this equality, the index k' has been introduced to refer to the four bonds where currents actually exist. Using (3.28) and (3.29), we obtain

$$ \frac{1}{\varepsilon_0} \sum_{k'=1}^{4} {}^{+}\lambda_{k'}^2 = \frac{1}{\mu_0} \sum_{k'=1}^{4} {}^{-}\lambda_{k'}^2 \tag{3.30} $$

where $\sum_{k'=1}^{4} {}^{+}\lambda_{k'}^2$ and $\sum_{k'=1}^{4} {}^{-}\lambda_{k'}^2$ do not depend on the node position.

To proceed further, we use the last symmetry we have not considered yet *i.e.* isotropy of the scattering process, which could be written as

$$ \forall k' = 1, \dots 4 \qquad {}^{+}\lambda_{k'}^2(\mathbf{r}) = {}^{+}\lambda^2 \tag{3.31a} $$

$$ \forall k' = 1, \dots 4 \qquad {}^{-}\lambda_{k'}^2(\mathbf{r}) = {}^{-}\lambda^2 \tag{3.31b} $$

where ${}^{+}\lambda^2$ (${}^{-}\lambda^2$) is the common value of the four ${}^{+}\lambda_{k'}^2(\mathbf{r})$'s (${}^{-}\lambda_{k'}^2(\mathbf{r})$'s) at node $\mathbf{r}$. Following our observation after (3.30), we note that ${}^{+}\lambda^2$ and ${}^{-}\lambda^2$ do not depend on the node position either. This property is expected since we consider a homogeneous system. Due to local inversion symmetry as stated by (3.13), we can rewrite (3.31a) and (3.31b) as

$$ \forall k' = 1, \dots 4 \qquad {}^{+}\lambda_{k'}(\mathbf{r}) = {}^{+}\lambda \tag{3.32a} $$

$$ \forall k' = 1, \dots 4 \qquad {}^{-}\lambda_{k'}(\mathbf{r}) = \delta_{k'}(\mathbf{r}) {}^{-}\lambda \tag{3.32b} $$

where the sign $\delta = \pm 1$ in (3.32b) depends on both $\mathbf{r}$ and k'. In particular, because of (3.13), we know that $\delta_{\overline{k'}}(\mathbf{r}) = -\delta_{k'}(\mathbf{r})$.

Having in mind the general definition (2.16) of the field $\Psi(\mathbf{r}, t)$, which becomes

$$ {}^{+}\Psi(\mathbf{r}, t) = \left({}^{+}\lambda / {}^{+}\Lambda_0\right) \sum_{k'=1}^{4} e_{k'}(\mathbf{r}, t) \tag{3.33a} $$

$$ {}^{-}\Psi(\mathbf{r}, t) = \left({}^{-}\lambda / {}^{-}\Lambda_0\right) \sum_{k'=1}^{4} \delta_{k'}(\mathbf{r}) e_{k'}(\mathbf{r}, t) \tag{3.33b} $$

we are free to choose ${}^{+}\lambda > 0$ and ${}^{-}\lambda > 0$ by setting the appropriate signs for the currents $e_{k'}(\mathbf{r}, t)$ accordingly.

Making use of (3.30) and (3.32), we obtain

$$ Z_0 = {}^{-}\lambda / {}^{+}\lambda \tag{3.34} $$

where $Z_0 = \sqrt{\mu_0/\varepsilon_0}$ is the vacuum impedance. Next, from (3.20) and (A.17) one can check that

$$ c_\nu \equiv 1/\sqrt{\varepsilon_0 \mu_0} = c_0/2 \tag{3.35} $$

Table 1. Coefficients ${}^{-}\lambda_k$ of the components H_x, H_y, and H_z along the six directions x, $\overline{x}$, y, $\overline{y}$, z and $\overline{z}$.

	x	$\overline{x}$	y	$\overline{y}$	z	$\overline{z}$
H_x	0	0	$-{}^{-}\lambda$	$+{}^{-}\lambda$	$+{}^{-}\lambda$	$-{}^{-}\lambda$
H_y	$+{}^{-}\lambda$	$-{}^{-}\lambda$	0	0	$-{}^{-}\lambda$	$+{}^{-}\lambda$
H_z	$-{}^{-}\lambda$	$+{}^{-}\lambda$	$+{}^{-}\lambda$	$-{}^{-}\lambda$	0	0

which relates the wave velocity c_ν in vacuum to the velocity c_0 of the currents. From (3.34) and (3.35), the permittivity and permeability of free space can be written as a function of the wave automaton parameters

$$ \varepsilon_0 = (2/c_0) {}^{+}\lambda / {}^{-}\lambda \tag{3.36a} $$

$$ \mu_0 = (2/c_0) {}^{-}\lambda / {}^{+}\lambda. \tag{3.36b} $$

The fact that ε_0 and μ_0 depend only on the ratio ${}^{-}\lambda / {}^{+}\lambda$ is reasonable since referring again to the definitions (3.33) of the fields, it is clear that ${}^{+}\lambda$ and ${}^{-}\lambda$ are defined modulo a multiplying factor through a scaling of the currents $e_{k'}$.

To complete the vacuum case, let us determine the sign $\delta_{k'}(\mathbf{r})$ of ${}^{-}\lambda_{k'}(\mathbf{r})$ in (3.32b). To achieve this task, we use (A.17) again. For instance, remembering the definition (3.20) of ${}^{\eta}t$, the first equality in (A.17), which reads

$$ {}^{+}\lambda_z[(2l+1)a, 2ma, (2n+1)a] {}^{-}\lambda_{\overline{z}}[(2l+1)a, 2ma, 2na] = {}^{+}\Lambda[(2l+1)a, 2ma, (2n+1)a]/[2\varepsilon_0 c_0] \tag{3.37} $$

becomes

$$ {}^{+}\lambda {}^{-}\lambda \delta_{\overline{z}}[(2l+1)a, 2ma, 2na] = 2 {}^{+}\lambda^2/[\varepsilon_0 c_0]. $$

Using (3.36a), we obtain

$$ \delta_{\overline{z}}[(2l+1)a, 2ma, 2na] = +1 $$

so that

$$ {}^{-}\lambda_{\overline{z}}[(2l+1)a, 2ma, 2na] = + {}^{-}\lambda \tag{3.38} $$

and using (3.13)

$$ {}^{-}\lambda_z[(2l+1)a, 2ma, 2na] = - {}^{-}\lambda. \tag{3.39} $$

Making use of (3.32a) and of the successive equalities in (A.17), it is straightforward to obtain the other signs $\delta_{k'}(\mathbf{r})$. The resulting $\lambda_{k'}(\mathbf{r})$'s are listed in Table 1.

These results complete the construction of the wave automaton for Maxwell's equations in vacuum. The coefficients ${}^{\eta}\lambda_k$ are all known so that the fields ${}^{\eta}\Psi$ and the scattering matrices are well defined according to (3.33) and (2.14) respectively. Let us now turn to the general case.

Table 2. Positions and λ_k values of the components E_x, E_y, and E_z, H_x, H_y, and H_z. The λ_k's must be multiplied by the scaling factor ${}^{+}\lambda$.

	E_x	E_y	E_z	H_x	H_y	H_z
x	$(2l+1)a$	$2la$	$2la$	$2la$	$(2l+1)a$	$(2l+1)a$
y	$2ma$	$(2m+1)a$	$2ma$	$(2m+1)a$	$2ma$	$(2m+1)a$
z	$(2n+1)a$	$(2n+1)a$	$2na$	$2na$	$2na$	$(2n+1)a$
λ_x	0	1	1	0	Z_0	$-Z_0$
$\lambda_{\overline{x}}$	0	1	1	0	$-Z_0$	Z_0
λ_y	1	0	1	$-Z_0$	0	Z_0
$\lambda_{\overline{y}}$	1	0	1	Z_0	0	$-Z_0$
λ_z	1	1	0	Z_0	$-Z_0$	0
$\lambda_{\overline{z}}$	1	1	0	$-Z_0$	Z_0	0
λ_7	$2\sqrt{\varepsilon_x-1}$	$2\sqrt{\varepsilon_y-1}$	$2\sqrt{\varepsilon_z-1}$	$2Z_0\sqrt{\mu_x-1}$	$2Z_0\sqrt{\mu_y-1}$	$2Z_0\sqrt{\mu_z-1}$

3.5.2 General case

We consider a medium characterized by the diagonal elements ε_i and μ_j of its permittivity and permeability tensors where $i,j \equiv x,y,z$. Focusing on the permittivity elements ε_i and introducing for convenience the following notation

$$
\begin{aligned}
{}^{+x}\lambda_7 &= {}^{+}\lambda_7[(2l+1)a, 2ma, (2n+1)a] \\
{}^{+y}\lambda_7 &= {}^{+}\lambda_7[2la, (2m+1)a, (2n+1)a] \\
{}^{+z}\lambda_7 &= {}^{+}\lambda_7[2la, 2ma, 2na].
\end{aligned}
$$

Equation (3.25) reads

$$
\begin{aligned}
[{}^{+}\Lambda_0 + {}^{+x}\lambda_7^2]/\varepsilon_0\varepsilon_x &= [{}^{+}\Lambda_0 + {}^{+y}\lambda_7^2]/\varepsilon_0\varepsilon_y \\
&= [{}^{+}\Lambda_0 + {}^{+z}\lambda_7^2]/\varepsilon_0\varepsilon_z \qquad (3.40)
\end{aligned}
$$

where we have used the definitions $\Lambda = \sum_{k=1}^{7}\lambda_k^2$ and (3.29).

Equation (3.40) clearly demonstrates that the value of the coefficient ${}^{+i}\lambda_7$ is related to the corresponding permittivity element ε_i. Since the values of the ε_i's are arbitrary, (3.40) must be valid in the particular case where one of the ε_i's equals one and the corresponding ${}^{+i}\lambda_7$ vanishes. Hence, we can write

$$
\begin{aligned}
[{}^{+}\Lambda_0 + {}^{+x}\lambda_7^2]/\varepsilon_0\varepsilon_x &= [{}^{+}\Lambda_0 + {}^{+y}\lambda_7^2]/\varepsilon_0\varepsilon_y \\
&= [{}^{+}\Lambda_0 + {}^{+z}\lambda_7^2]/\varepsilon_0\varepsilon_z = {}^{+}\Lambda_0/\varepsilon_0 \qquad (3.41)
\end{aligned}
$$

which leads to

$$
\varepsilon_i = 1 + {}^{+i}\lambda_7^2/{}^{+}\Lambda_0 \qquad i = x,y,z. \qquad (3.42)
$$

Since ${}^{+}\Lambda_0 = 4{}^{+}\lambda^2$ according to (3.29) and (3.32a), we can rewrite (3.42) as

$$
{}^{+i}\lambda_7/{}^{+}\lambda = 2\sqrt{\varepsilon_i - 1} \qquad i = x,y,z \qquad (3.43)
$$

which expresses ${}^{+i}\lambda_7$ as a function of ε_i.

Using (3.25) again for the permeability elements μ_j, it is straightforward to find

$$
\mu_j = 1 + {}^{-j}\lambda_7^2/{}^{-}\Lambda_0 \qquad j = x,y,z \qquad (3.44)
$$

$$
{}^{-j}\lambda_7/{}^{-}\lambda = 2\sqrt{\mu_j - 1} \qquad j = x,y,z \qquad (3.45)
$$

where

$$
\begin{aligned}
{}^{-x}\lambda_7 &= {}^{-}\lambda_7[2la, (2m+1)a, 2na] \\
{}^{-y}\lambda_7 &= {}^{-}\lambda_7[(2l+1)a, 2ma, 2na] \\
{}^{-z}\lambda_7 &= {}^{-}\lambda_7[(2l+1)a, (2m+1)a, (2n+1)a].
\end{aligned}
$$

Together with (3.32a) and (3.32b), equations (3.43, 3.45) determine the whole set of the λ_k's values, which are listed in Table 2. In the next section, we summarize the results for any material characterized by its permittivity and permeability diagonal elements.

3.6 Fields and scattering matrices of the Maxwell wave automaton

In this section, we write the expressions of the fields and scattering matrices as a function of the material parameters ε_x, ε_y, ε_z and μ_x, μ_y, μ_z. For that, we use the definition (2.16) of the fields Ψ, equation (2.14) for the scattering elements d_{kl} and the values of the λ_k's listed in Table 2.

Let i, j, and k to be any circular permutation of x, y and z. The electric and magnetic fields E_i and H_i are given by

$$
E_i \equiv {}^{+i}\Psi = \left(e_j + e_{\overline{j}} + e_k + e_{\overline{k}} + 2\sqrt{\varepsilon_i - 1}\, e_7\right)/4\varepsilon_i {}^{+}\lambda \qquad (3.46)
$$

$$
\begin{aligned}
H_i &\equiv {}^{-i}\Psi \\
&= \left(-e_j + e_{\overline{j}} + e_k - e_{\overline{k}} + 2\sqrt{\mu_i - 1}\, e_7\right)/4\mu_i Z_0 {}^{+}\lambda. \qquad (3.47)
\end{aligned}
$$

$$D_E = 1/\varepsilon_i \begin{pmatrix} 1/2-\varepsilon_i & 1/2 & 1/2 & 1/2 & \sqrt{\varepsilon_i-1} \\ 1/2 & 1/2-\varepsilon_i & 1/2 & 1/2 & \sqrt{\varepsilon_i-1} \\ 1/2 & 1/2 & 1/2-\varepsilon_i & 1/2 & \sqrt{\varepsilon_i-1} \\ 1/2 & 1/2 & 1/2 & 1/2-\varepsilon_i & \sqrt{\varepsilon_i-1} \\ \sqrt{\varepsilon_i-1} & \sqrt{\varepsilon_i-1} & \sqrt{\varepsilon_i-1} & \sqrt{\varepsilon_i-1} & \varepsilon_i-2 \end{pmatrix} \tag{3.48}$$

$$D_H = 1/\mu_i \begin{pmatrix} -1/2+\mu_i & 1/2 & 1/2 & -1/2 & \sqrt{\mu_i-1} \\ 1/2 & -1/2+\mu_i & -1/2 & 1/2 & -\sqrt{\mu_i-1} \\ 1/2 & -1/2 & -1/2+\mu_i & 1/2 & -\sqrt{\mu_i-1} \\ -1/2 & 1/2 & 1/2 & -1/2+\mu_i & \sqrt{\mu_i-1} \\ \sqrt{\mu_i-1} & -\sqrt{\mu_i-1} & -\sqrt{\mu_i-1} & \sqrt{\mu_i-1} & 2-\mu_i \end{pmatrix} . \tag{3.49}$$

The associated scattering matrices D_E and D_H read

see equations (3.48, 3.49) above.

Note that the coefficient ${}^{+}\lambda$ appears in the expression (3.46) and (3.47) of the fields since the currents are defined modulo an arbitrary multiplying constant. In contrast, the scattering matrices cannot depend on this scaling factor, as confirmed by (3.48) and (3.49). Last, let us remind that the locations of the field components E_i and H_i, $i = x, y, z$ are given in Table 2.

4 Discussion and conclusion

In the spirit of the previous versions of the wave automaton devoted to scalar [6,14] or spinor [15] wave propagation, we have described a wave automaton capable of modeling Maxwell's equations in the time domain. As several Maxwell's equations solvers have been introduced for a long time, it is important to compare our results with other methods. The Maxwell wave automaton shares common features essentially with three other algorithms, namely cellular automata [8], the TLM method [18] and the FDTD method [19,20]. Therefore, it will be compared with those three methods successively.

Cellular automata have been developed for many years to simulate the behavior of complex systems. A special class of cellular automata termed lattice gas automata has been devoted to fluid dynamics. They are defined by particles moving in discrete time steps from node to node of a discrete lattice. At each node, the particles experience collisions according rules, which mimic the collisions of classical particles. The basic propagation and scattering rules of the wave automaton are very similar. However, in contrast with the wave automaton, the particles of cellular automata are described by Boolean variables allowing the use of low precision arithmetic. Due to this feature and to their collision rules, their application to partial differential equations concerns essentially the Navier-Stokes equation of hydrodynamics. Quite recently, a lattice gas automaton using binary variables has been introduced to describe the three-dimensional electromagnetic fields [13]. Successful simulations of resonant frequencies within various cavities have validated this attempt. However, in contrast with the wave automaton, this lattice gas automaton has not yet been analytically proven to be equivalent to Maxwell's equations. In the last few years, the lattice Boltzmann method [8], which is an extension of cellular automata from Boolean to real numbers dynamics, has been successfully used to describe wave propagation from first principles [7]. However, until now, such attempts have been limited to the scalar wave equation.

The method to which the wave automaton bears most resemblance is the TLM method. Both methods rely on a discrete equivalent of Huygens' principle. In particular, although they do not refer to any *a priori* electromagnetic property, one can think of the wave automaton currents as equivalent to the voltage pulses in TLM. Moreover, one of the most appealing features in TLM originates in the use of passive electrical networks, which guarantees the numerical stability of TLM algorithms. While this is not as obvious as in TLM, we have shown that stability is also one of the main properties of the wave automaton. This is due to the fact that the scattering matrices are orthogonal, a property that results from time reversal symmetry and reciprocity. Hence, even though both methods differ in their foundations, one can wonder whether the resulting algorithms are identical. In particular, are the scattering matrices the same in both methods? To make such a comparison, let us first recall that several algorithms, which rely on the usage of different nodes, have been developed in TLM to describe 3D electromagnetic fields, the most popular being the symmetrical condensed node (SCN) [21]. Among those different

algorithms, the expanded node, which is made of interweaving shunt and series two-dimensional nodes [22], has been used extensively before the advent of the SCN node. Like the Maxwell wave automaton, its geometry is the Yee cell. Hence, the Maxwell wave automaton can only be compared with the expanded node TLM algorithm. In this algorithm, the scattering matrices are associated to the shunt and series two-dimensional nodes, which represent the electric and magnetic field components respectively. We do not reproduce here those scattering matrices, which are well known in the TLM literature [23]. Comparison with D_E (Eq. (3.48)) and D_H (Eq. (3.49)) shows that the wave automaton scattering matrices actually differ from the TLM ones. In particular, the TLM scattering matrices are not symmetrical, not either orthogonal except in the case of vacuum ($\varepsilon_i = 1$ and $\mu_i = 1$) where they become identical to the wave automaton ones. Hence, although they are strongly akin, the wave automaton and TLM methods are surprisingly different. As pointed out above, TLM can use different algorithms to describe 3D electromagnetic fields. Hence, one can wonder whether it is possible to find appropriate TLM nodes that are described by the wave automaton scattering matrices D_E and D_H. We are not aware of the existence of such nodes at the present time.

Finally, how does the wave automaton compare with the FDTD method? At first sight, both methods are different in their foundations. The FDTD method results from finite- difference expressions for the space and time derivatives of the Maxwell's equations in the Yee cell geometry. In contrast, the Maxwell wave automaton results from the time evolution of the currents, which mimic a discrete Huygens'principle. However, we have shown that by introducing appropriate field definitions and fundamental physical symmetries, the wave automaton also describes the FDTD discrete equations in the Yee cell geometry. Hence, both methods are equivalent.

To recapitulate, while the Maxwell wave automaton shares the same modeling philosophy as the cellular automata or the TLM method, it has been shown that it is only strictly equivalent to the FDTD method. This equivalence calls for some observations. First, any solution of an electromagnetic investigation in the time domain using the wave automaton approach is bound to give results identical to those obtained with FDTD. Obviously, the Maxwell wave automaton is still in the infancy and does not benefit from the numerous developments of the FDTD method. For instance, this wave automaton has been shown to be equivalent to the second-order finite-difference scheme by Yee. A question that can be posed is, which modifications should be brought in the derivation of the model to obtain higher order finite-difference schemes. We have no clue at the moment for such better schemes. In order to bring up the wave automaton to the status of a versatile Maxwell's equations solver like FDTD or TLM, many improvements are still to be introduced such as dissipation, dispersion or absorbing boundary conditions to cite a few ones. However, its present status already enables one to solve electromagnetic propagation in *inhomogeneous* and *anisotropic* media. Next, because of this equivalence, it is legitimate to ask for the benefits to be expected from the Maxwell wave automaton when compared to FDTD or other methods. As a numerical tool to solve Maxwell's equations, it does not bring at this stage of development any new advantage in precision or speed. Its more apparent practical advantages are the same as the attractive features of cellular automata and TLM, namely stability and the intuitive and easy way to write programs respectively. Especially, it is well adapted to parallel architectures since the time evolution of the currents only involves local scattering and propagation to nearest neighbors. Actually, the main interest in the wave automaton is not practical but conceptual. It is remarkable that the simple picture of current's scattering and propagation with appropriate fundamental symmetries, which was already introduced in the past to rebuild the scalar wave equation [6,14] is still effective for the more complicated case of the 3D Maxwell's equations. This result might seem to be obvious since it is well known that Huygens' principle is contained in Maxwell's equations. However, the rather lengthy developments of this paper show that the link between the discrete equivalents of Huygens'principle and of the Maxwell's equations is not straightforward. In particular, we are not aware of any retrieval of finite difference algorithms for Maxwell' equations straight from physical principles as was done in the present work rather than from the classical discretization of the continuous equations using the standard mathematical methods that are well-known in numerical PDEs. The only attempt brought to our knowledge is the lattice gas automaton described in [13]. However, as pointed out before, this automaton has not been proven yet to be equivalent to Maxwell's equations.

Eventually, the advantage of the wave automaton picture of Maxwell's equations is expected to manifest itself in providing intuitive answers to questions raised in specific applications. To illustrate this point, let us focus our attention on dissipation, which was not considered in this paper. In FDTD, dissipation is handled by taking into account electric and magnetic conductivities. In the wave automaton, there are several ways to impose losses. The most intuitive ones are to introduce damping factors in the propagation or the scattering step of the currents. Preliminary results show that this procedure is equivalent to introducing correlated electric and magnetic conductivities in the resulting finite difference equations. Further work is needed to explore and compare the consequences of these different possibilities. Similar intuitive pictures can be considered in order to introduce dispersion or absorbing boundary conditions. The hope is not only to retrieve in a simple way the techniques already known in FDTD or TLM, but also to shed new light over those techniques in the frame of the discrete Huygens'principle. Hopefully, new schemes are expected to emerge from this approach.

The author wishes to thank O. Legrand, F. Mortessagne and P. Sebbah for useful discussions and for a critical reading of the manuscript.

$$
\begin{aligned}
{}^{+}\Psi[(2l+1)a, 2ma, (2n+1)a] &\equiv E_x[(2l+1)a, 2ma, (2n+1)a] \\
{}^{+}\Psi[2la, (2m+1)a, (2n+1)a] &\equiv E_y[2la, (2m+1)a, (2n+1)a] \\
{}^{+}\Psi[2la, 2ma, 2na] &\equiv E_z[2la, 2ma, 2na] \\
{}^{-}\Psi[2la, (2m+1)a, 2na] &\equiv H_x[2la, (2m+1)a, 2na] \\
{}^{-}\Psi[(2l+1)a, 2ma, 2na] &\equiv H_y[(2l+1)a, 2ma, 2na] \\
{}^{-}\Psi[(2l+1)a, (2m+1)a, (2n+1)a] &\equiv H_z[(2l+1)a, (2m+1)a, (2n+1)a]
\end{aligned} \tag{A.16}
$$

Appendix

In this appendix, we identify the wave automaton equations (3.22) with the Maxwell's equations (3.23). Let us compare equations (3.22a, 3.23a) for the case of the component E_x, *i.e.*

$$ {}^{+}\Psi[\mathbf{r}] = E_x[\mathbf{r}] \tag{A.1} $$

at nodes $\mathbf{r} = \{(2l+1)a, 2ma, (2n+1)a\}$ and

$$ {}^{-}\Psi[\mathbf{r}] = H_z[\mathbf{r}] \tag{A.2} $$

$$ {}^{-}\Psi[\mathbf{r}] = H_y[\mathbf{r}] \tag{A.3} $$

at neighbor nodes $\{(2l+1)a, (2m+1)a, (2n+1)a\}$ and $\{(2l+1)a, 2ma, 2na\}$ respectively. Moreover, we must have

$$
-\frac{2c_0\,{}^{+}t_y[(2l+1)a, 2ma, (2n+1)a]}{{}^{+}\Lambda[(2l+1)a, 2ma, (2n+1)a]} = \\
+\frac{2c_0\,{}^{+}t_z[(2l+1)a, 2ma, (2n+1)a]}{{}^{+}\Lambda[(2l+1)a, 2ma, (2n+1)a]} = \frac{1}{\varepsilon_0\varepsilon_x}\cdot \tag{A.4}
$$

Hence,

$$
{}^{+}t_z[(2l+1)a, 2ma, (2n+1)a] = \\
-{}^{+}t_y[(2l+1)a, 2ma, (2n+1)a]. \tag{A.5}
$$

A peculiarity of the Yee cell geometry is that some nodes are vacant. For instance, the nodes E_x have no neighbor components H_j along the x direction. Accordingly, we shall set that the field ${}^{-}\Psi(\mathbf{r})$ is not defined for $\mathbf{r} = \{2la, 2ma, (2n+1)a\}$. Hence, we write that the corresponding ${}^{-}\lambda_k$'s vanish

$$ {}^{-}\lambda_k[2la, 2ma, (2n+1)a] = 0 \qquad \forall k = 1, 2, \dots 7 \tag{A.6} $$

and that no currents propagate to or from nodes $\{2la, 2ma, (2n+1)a\}$. In particular, there are no currents along the x axis that contributes to the definition of the field ${}^{+}\Psi \equiv E_x$ at nodes $\mathbf{r} = \{(2l+1)a, 2ma, (2n+1)a\}$. Hence, we write

$$ {}^{+}\lambda_k[(2l+1)a, 2ma, (2n+1)a] = 0 \qquad k = x, \overline{x}. \tag{A.7} $$

Instead of seven currents, only five incident currents e_k at nodes $\mathbf{r} = \{(2l+1)a, 2ma, (2n+1)a\}$ enter the definition of ${}^{+}\Psi$, which reads

$$
{}^{+}\Psi(\mathbf{r}) \equiv E_x(\mathbf{r}) = \lambda_y(\mathbf{r})[e_y(\mathbf{r}) + e_{\overline{y}}(\mathbf{r})] \\
+\lambda_z(\mathbf{r})[e_z(\mathbf{r}) + e_{\overline{z}}(\mathbf{r})] + \lambda_7(\mathbf{r})e_7(\mathbf{r}). \tag{A.8}
$$

From (A.6) or (A.7), we also obtain

$$ {}^{-}t_k[2la, 2ma, (2n+1)a] = 0 \qquad \forall k = 1, 2, \dots 7 \tag{A.9} $$

$$
{}^{+}t_x[(2l+1)a, 2ma, (2n+1)a] = \\
{}^{+}t_{\overline{x}}[(2l+1)a, 2ma, (2n+1)a] = 0. \tag{A.10}
$$

The identification of other components is similar. Before providing the final results, it is worth making a few remarks about the way to obtain them. First, at any vacant node (see Fig. 4), the corresponding ${}^{\eta}\lambda_k$ will vanish. Hence, in addition to (A.6), one finds

$$ {}^{+}\lambda_k[(2l+1)a, (2m+1)a, 2na] = 0 \qquad \forall k = 1, 2, \dots 7 \tag{A.11} $$

and accordingly

$$ {}^{+}t_k[(2l+1)a, (2m+1)a, 2na] = 0 \qquad \forall k = 1, 2, \dots 7. \tag{A.12} $$

Next, according to their definition (3.20), the parameters t_k verify

$$ {}^{\eta}t_k(\mathbf{r}) = {}^{-\eta}t_{\overline{k}}(\mathbf{r}_k). \tag{A.13} $$

As a consequence, knowing ${}^{\eta}t_k$ at some node $\mathbf{r}$ provides immediately the values ${}^{-\eta}t_{\overline{k}}$ at its neighbor nodes $\mathbf{r}_k$. Knowing ${}^{-\eta}t_{\overline{k}}(\mathbf{r}_k)$, we also get ${}^{-\eta}t_k(\mathbf{r}_k)$ since

$$ {}^{-\eta}t_k(\mathbf{r}_k) = -\eta\,{}^{-\eta}t_{\overline{k}}(\mathbf{r}_k) \tag{A.14} $$

which follows from (3.20) and (3.13). Last, at each node, one finds an equation similar to (A.5), *i.e.* the two non zero values ${}^{\eta}t_k$ and ${}^{\eta}t_l$ along two perpendicular directions k and l verify

$$ {}^{\eta}t_k = \pm{}^{\eta}t_l. \tag{A.15} $$

Eventually, we obtain the following set of identities

see equation (A.16) above

and

$$
\begin{aligned}
{}^{+}t_z[(2l+1)a, 2ma, (2n+1)a] = \\
{}^{+}\Lambda[(2l+1)a, 2ma, (2n+1)a]/[2\varepsilon_0\varepsilon_x c_0] \\
= -{}^{+}t_y[(2l+1)a, 2ma, (2n+1)a] \\
= +{}^{+}t_x[2la, (2m+1)a, (2n+1)a] \\
= {}^{+}\Lambda[2la, (2m+1)a, (2n+1)a]/[2\varepsilon_0\varepsilon_y c_0] \\
= -{}^{+}t_z[2la, (2m+1)a, (2n+1)a] \\
= +{}^{+}t_y[2la, 2ma, 2na] \\
= {}^{+}\Lambda[2la, 2ma, 2na]/[2\varepsilon_0\varepsilon_z c_0] \\
= -{}^{+}t_x[2la, 2ma, 2na] \\
= +{}^{-}t_z[2la, (2m+1)a, 2na] \\
= {}^{-}\Lambda[2la, (2m+1)a, 2na]/[2\mu_0\mu_x c_0] \\
= -{}^{-}t_y[2la, (2m+1)a, 2na] \\
= +{}^{-}t_x[(2l+1)a, 2ma, 2na] \\
= {}^{-}\Lambda[(2l+1)a, 2ma, 2na]/[2\mu_0\mu_y c_0] \\
= -{}^{-}t_z[(2l+1)a, 2ma, 2na] \\
= +{}^{-}t_y[(2l+1)a, (2m+1)a, (2n+1)a] \\
= {}^{-}\Lambda[(2l+1)a, (2m+1)a, (2n+1)a]/[2\mu_0\mu_z c_0] \\
= -{}^{-}t_x[(2l+1)a, (2m+1)a, (2n+1)a] \quad \text{(A.17)}
\end{aligned}
$$

to which we must add (A.6, A.11) and

$$
\begin{aligned}
{}^{+}t_x[(2l+1)a, 2ma, (2n+1)a] = 0 \\
{}^{+}t_y[2la, (2m+1)a, (2n+1)a] = 0 \\
{}^{+}t_z[2la, 2ma, 2na] = 0 \\
{}^{-}t_x[2la, (2m+1)a, 2na] = 0 \\
{}^{-}t_y[(2l+1)a, 2ma, 2na] = 0 \\
{}^{-}t_z[(2l+1)a, (2m+1)a, (2n+1)a] = 0. \quad \text{(A.18)}
\end{aligned}
$$

Although equations (3.22) are now fully identical to Maxwell's equations (3.23), the construction of the wave automaton is not completed since most of the λ_k's remain unknown. At this stage, we only know the λ_k's that are equal to zero at the vacant sites according to (A.6) and (A.11). Moreover, according to (A.18) we can also write

$$
\begin{aligned}
{}^{+}\lambda_x[(2l+1)a, 2ma, (2n+1)a] = 0 \\
{}^{+}\lambda_y[2la, (2m+1)a, (2n+1)a] = 0 \\
{}^{+}\lambda_z[2la, 2ma, 2na] = 0 \\
{}^{-}\lambda_x[2la, (2m+1)a, 2na] = 0 \\
{}^{-}\lambda_y[(2l+1)a, 2ma, 2na] = 0 \\
{}^{-}\lambda_z[(2l+1)a, (2m+1)a, (2n+1)a] = 0. \quad \text{(A.19)}
\end{aligned}
$$

The values of the other λ_k's are obtained in the main text by using the implicit equations (A.17).

From (A.17), we immediately obtain

$$
\begin{aligned}
{}^{+}\Lambda[(2l+1)a, 2ma, (2n+1)a]/\varepsilon_0\varepsilon_x = \\
{}^{+}\Lambda[2la, (2m+1)a, (2n+1)a]/\varepsilon_0\varepsilon_y \\
= {}^{+}\Lambda[2la, 2ma, 2na]/\varepsilon_0\varepsilon_z \quad \text{(A.20)} \\
= {}^{-}\Lambda[2la, (2m+1)a, 2na]/\mu_0\mu_x \\
= {}^{-}\Lambda[(2l+1)a, 2ma, 2na]/\mu_0\mu_y \\
= {}^{-}\Lambda[(2l+1)a, (2m+1)a, (2n+1)a]/\mu_0\mu_z
\end{aligned}
$$

which are reported to as equations (3.25) in Section 3.4.

References

1. C. Vanneste, P. Sebbah, D. Sornette, Europhys. Lett. **17**, 715 (1992); **18**, 567 (1993) (Erratum).
2. P. Sebbah, D. Sornette, C. Vanneste, J. Phys. I France **3**, 1259 (1993); J. Phys. I France **3**, 1281 (1993).
3. P. Enders, Eur. J. Phys. **17**, 226 (1996).
4. W.J.R. Hoefer, *Huygens and the Computer - A Powerful Alliance in Numerical Electromagnetics, Proc. IEEE 79, 1459 (1991)* and references cited therein.
5. D. Sornette, O. Legrand, F. Mortessagne, P. Sebbah, C. Vanneste, Phys. Lett. A **178**, 292 (1993).
6. S. de Toro Arias, C. Vanneste, J. Phys. I France **7**, 1071 (1997).
7. B. Chopard, P.O. Luthi, J.-F. Wagen, IEE Proc.-Microw. Antennas Propag. **144**, 251 (1997).
8. B. Chopard, M. Droz, *Cellular Automata Modeling of Physical Systems* (Cambridge University Press, 1998) and references therein.
9. B.M. Boghosian, W. Taylor, *Simulating Quantum Mechanics on a Quantum Computer*, BU-CCS-970103, preprint `quant-ph/9604035`, talk presented at *the PhysComp '96, Boston University, Boston, November 1996.*
10. D. Meyer, J. Stat. Phys. **85**, 551 (1996).
11. B. Shapiro, Phys. Rev. Lett. **48**, 823 (1982).
12. P. Freche, M. Janssen, R. Merkt, Phys. Rev. Lett. **82**, 149 (1999).
13. N.R.S. Simons, G.E. Bridges, M. Cuhaci, J. Comput. Phys. **151**, 816 (1999).
14. O. Legrand, F. Mortessagne, P. Sebbah, C. Vanneste, J. Comput. Phys. **160**, 541 (2000).
15. S. de Toro Arias, C. Vanneste, Eur. Phys. J. B **3**, 517 (1998).
16. K.S. Yee, IEEE Trans. Antennas Propagation. **14**, 302 (1966).
17. Complex instead of real currents should be introduced for other wave equations such as the Schrödinger equation. See [6] for instance.
18. C. Christopoulos, *The Transmission Line Modelling Method* (IEEE Press, Piscataway, NJ, 1993).
19. K. Kunz, R. Luebbers, *The Finite Difference Time Domain Method for Electromagnetics* (CRC Press, Boca Raton, Florida, 1993).
20. A. Taflove, *Computational Electrodynamics: The Finite-Difference Time-Domain Method* (Artech House, Norwood, MA, 1995).
21. P.B. Johns, Electronic Lett. **22**, 162 (1986).
22. S. Akhtarzad, P.B. Johns, *Proceedings of IEE* **122**, 1344 (1975).
23. See for instance, chapter 5 in [18].